



Contents lists available at ScienceDirect

Quaternary International

journal homepage: www.elsevier.com/locate/quaint

A 4000-yr multi-proxy record of Holocene hydrology and vegetation from a peatland in the Sanjiang Plain, Northeast China

Hanxiang Liu ^{a, b}, Xiaofei Yu ^{a, **}, Chuanyu Gao ^a, Zhenqing Zhang ^a, Chunling Wang ^c, Wei Xing ^{a, b}, Guoping Wang ^{a, *}

^a Key Laboratory of Wetland Ecology and Environment, Northeast Institute of Geography and Agroecology, Chinese Academy of Sciences, Changchun, 130102, China

^b University of Chinese Academy of Sciences, Beijing, 100049, China

^c College of Urban and Rural Construction, ShanXi Agricultural University, Jinzhong, 030801, China

ARTICLE INFO

Article history:

Received 11 October 2016

Received in revised form

18 December 2016

Accepted 25 December 2016

Available online xxx

Keywords:

Holocene

Multi-proxy

Vegetation

Water level

Indicator sensitivity

Peatland

ABSTRACT

Reconstructing historical hydrologic and vegetation conditions can provide useful insights into the mechanisms underlying peatland development and can be used to construct baselines for peatland restoration. In this study, we present numerous physical and biological indices for a 4000-year core from the Honghe National Natural Reserve (HE), a dish-like depression peatland in the Sanjiang Plain of Northeast China. The history of vegetation change was reconstructed by combining plant macrofossils and pollen data from the core, and the water level changes were reconstructed through a multi-proxy study of plant macrofossils, charcoal, stable carbon isotopes, testate amoebae, sediment grain size, loss on ignition, humification degree and magnetic susceptibility. We found that the HE peatland featured wet condition from 4000 to 3600 cal yr BP, which was in accordance with the extreme flooding event at 4.0 ka in northern China. Significant drier shifts were recorded at 3600 and 1200 cal yr BP, while significant wetter shifts were recorded at 2600 and 500 cal yr BP. Factor analysis were applied to all of the proxies to reduce the seven variables to two factors, and the biological indicators, such as plant macrofossils, charcoal and stable carbon isotopes, were found to be more sensitive than the other parameters to water level changes over the last 4000 years. Furthermore, the multi-proxy reconstruction of the wetness of the HE peatland resembles the pattern observed at other sites in Northeast China.

© 2016 Elsevier Ltd and INQUA. All rights reserved.

1. Introduction

Many ecological and environmental scientists are interested in peatland paleohydrology and paleovegetation. Among other indicators, testate amoebae (Charman et al., 1999; Elliott et al., 2012), charcoal (Lejju, 2009; Zhang et al., 2015b), stable carbon isotopes (Bohra and Kotlia, 2015), humification degree (HD) (Baker et al., 1999; Wang et al., 2015), loss on ignition (LOI) (Mansell et al., 2014), grain size (Kotlia et al., 2010; Zhang et al., 2014), and magnetic mineralogy (Kotlia et al., 2010; Onac et al., 2015) have been used as indicators of historic peatland surface wetness. Among other plant derivatives, plant macrofossils (Barber et al., 1994; Plunkett and Swindles, 2008; Wang et al., 2015), pollen (Janssens,

1983; Zhang et al., 2015b), and phytoliths (Benvenuto et al., 2013; Pawlowski et al., 2015) have been used as indicators of historic vegetation. Based on this information, we can understand the mechanisms associated with peatland development and construct baselines for peatland restoration based on the reconstructed hydrology, vegetation and other aspects of physico-chemical quality. Because the use of a single proxy may produce erroneous interpretations, the use of a multi-proxy approach is valuable for assessing hydro-climatic changes and comparing the validity of different proxies (Blundell and Barber, 2005). Multi-proxy analysis of sediment core from lake was used to gain better understanding of regional climatic changes since the Late Quaternary (Argollo and Mourguiart, 2000; Henderson and Holmes, 2009; Shen et al., 2005). The peatlands are more readily and economically cored than lake bottom, and their autochthonous mode of accumulation renders them less susceptible to the redeposition that can bedevil some lake-sediment sequences (Chambers and Charman, 2004). Therefore, the peat-based multi-proxy analyses are deserving of greater

* Corresponding author.

** Corresponding author.

E-mail addresses: yuxf@iga.ac.cn (X. Yu), wangguoping@iga.ac.cn (G. Wang).

attention from the researchers.

Wetlands in the Sanjiang Plain in Northeast China have suffered a sharp decline since the 1950s due to large-scale land reclamation. Reclaiming and destroying forests, grasslands and wetlands has led to a series of ecological problems, such as the loss of biodiversity, an increase in soil erosion and the intensification of pollution by agricultural chemicals (Liu and Ma, 2000). To protect the regional environment, it is necessary to restore wetland ecosystems, and reconstructing the historical hydrology and vegetation is a key component of the ecological restoration of the wetlands (Liu et al., 2016). Dish-like depression peatlands are one of the most common types of wetlands in the Sanjiang Plain. The weather and climate of the Sanjiang Plain are mainly shaped by the East Asian monsoon, and the area is sensitive to climatic changes due to its mid-high latitudes and its location at the margins of the monsoon zone (An, 2000). Therefore, this region is well suited for tracking the historical changes in hydrology and vegetation. However, there are few well-dated, multi-proxy records from peatlands in the Sanjiang Plain, and our study represents the first high-resolution multi-proxy paleoecological investigation of the Sanjiang Plain in Northeast China.

In this study, we conduct a comprehensive analysis of plant macrofossils, testate amoebae, charcoal, HD, LOI, grain size, stable carbon isotopes and magnetic susceptibility to reconstruct the history of water level changes, and we combine plant macrofossils and pollen data to reconstruct the historical vegetation succession in the Honghe (HE) peatland of the Sanjiang Plain. The objectives of this study are to (1) reconstruct the paleohydrology and paleovegetation over the past 4000 years using a multi-proxy approach, (2) assess the sensitivity of each proxy, and (3) compare our paleohydrology information with that of other studies.

2. Study area

The Sanjiang Plain is located in northeast Heilongjiang Province, China. It is a large, low, flat alluvial plain with a total area of $10.89 \times 10^4 \text{ km}^2$, a mean elevation of 45–60 m, and a slope grade of less than 1:5000. The present climate is temperate monsoon with a mean annual temperature of 1.4–4.3 °C, and the average maximum and minimum temperatures are 22 °C in July and –21 °C in January, respectively. The mean annual precipitation is 500–550 mm, and 60% of the rainfall occurs between June and August. The main soil types are black soil, bleached soil, meadow soil, boggy soil, among which the meadow and boggy soils are the most widely distributed (Liu and Ma, 2002). Because of its special topography and climate, a large number of wetlands have developed in this area. A recent study shows that over 70% of the plain was once dominated by freshwater wetlands that develop in ancient riverbeds and water-logged depressions (Zhang et al., 2015a). The digital elevation model map of the Sanjiang Plain and the coring location can be found in Zhang et al. (2015b) and Wang et al. (2016).

3. Materials and methods

3.1. Fieldwork

A master core (47°47′20.10″N, 133°37′39.36″E) was obtained with a 5-cm × 50-cm Russian corer from the central area of the HE peatland, which is located in the northern part of the Sanjiang Plain. The profile was cut into contiguous 1-cm samples in the field using a stainless steel knife, and a total of 148 samples were extracted. The thickness of the peat layer was 115 cm (18–133 cm). The samples were sealed in tagged plastic bags for transport to the laboratory and refrigerated at 4 °C for further analysis.

3.2. Physical parameters analysis

Peat subsamples of 0.125 g dry weight were taken from each core sample at 1-cm intervals to determine the HD, which was measured using a chemical extraction technique at the Analysis and Test Center of the Northeast Institute of Geography and Agroecology (IGA) of the Chinese Academy of Sciences (CAS). After extraction with 8% NaOH and filtration, the light absorbance of the solution was measured using a UV-2500 visible spectrophotometer with a 540 nm filter. The HD was characterized as the mean percentage of the absorbance values of three replicated samples. The raw HD data were detrended using the following equation (Blundell and Barber, 2005):

$$Z = \frac{X - \mu}{\sigma} \quad (1)$$

(Z = detrended value; X = raw value; μ = mean of all X; and σ = standard deviation of X).

The LOI analysis samples were dried in an oven at 105 °C for 12 h and burnt at 550 °C in a muffle for 4 h following the procedures of Heiri et al. (2001) and Santisteban et al. (2004). The LOI value was calculated as the percentage of the initial weight that burned away.

The subsamples used to determine grain size were prepared following the method used by Zhang et al. (2014), and the grain sizes were measured with a Mastersizer 2000 laser grain-size analyzer (Malvern Instruments Ltd, Malvern, Worcestershire, UK) following the method described by Lu and An (1998).

For the analysis of magnetic susceptibility, subsamples were dried to a constant weight at normal atmospheric temperature and ground into a powder. Magnetic susceptibility was determined using a Bartington Instruments Ltd. MS2 meter at low frequency, 0.46 kHz, to calculate mass magnetic susceptibility (χ_{lf}). All of the above physical parameters were analyzed at the Analysis and Test Center of IGA, CAS.

3.3. Stable carbon isotopes

The roots of the sedges, *Drepanocladus aduncus* Warnst and *Equisetum hiemale* were collected from samples from between the depths of 1–14 cm, 16–90 cm, and 92–148 cm, respectively, and rinsed several times with deionized water until the solution reached a neutral pH. The stable carbon isotope analysis was conducted using a MAT 253 stable isotope ratio mass spectrometer (Thermo Fisher Scientific, New York, America) at the Analysis and Test Center of IGA, CAS.

3.4. The comprehensive analysis of plant macrofossils, pollen and charcoal

Plant macrofossils were analyzed using the quadrat and leaf count protocol (Barber et al., 1994) to investigate changes in the species composition of the vegetation during wetland development. Seeds, ericaceous leaves and charcoal were counted as absolute numbers, and the methods for preparing the subsamples and the details of the species identification can be found in Wang et al. (2016). Detrended correspondence analysis (DCA) was applied to the plant macrofossil data using CANOCO 4.5 to define the latent environment gradients (Barber et al., 1994), and the values of the main axis 1 were plotted against the age model to obtain a proxy climate record over time. A method based on that of Faegri et al. (1989) was used in the pollen analysis, in which a known number of *Lycopodium* spores were added to the samples. The sample preparation and pollen identification are detailed in Zhang et al. (2015b). The pollen and plant macrofossil diagram was created by

R software (v3.0.3) using the rioja library package. The changes in the species composition of the vegetation were then shown in the diagram, and the plant zones were determined by cluster analysis. The final charcoal data was determined by the mean values of the absolute numbers of the charcoal counted in both plant macrofossils and pollen samples.

3.5. Factor analysis

Factor analysis can reduce or simplify data by extracting eigenvalues and eigenvectors from a covariance or correlation matrix (Davis and Sampson, 1986). We used this method to identify the associations between all proxies, to explore the basic structure of the proxy data and to show the basic data structure for several factors. The reverse proxies, such as grain size and magnetic susceptibility, were converted to positive index values by adding a minus before the factor analysis. Principal component analysis was used as the extraction method, and conducted in SPSS 19, and the number of factors was determined by the eigenvalues that were greater than 1 (Kaiser, 1960). To identify the proxies that were most significant for each factor, we applied varimax orthogonal rotation to the component matrix (Buckley et al., 1995; Davis and Sampson, 1986), and the principal component factor scores and integrated scores of the varimax rotation were then calculated. The factor scores transformed the proxy data to a range of variations without changing the original trend in the variation in the data (Bai et al., 2012). Therefore, the integrated scores could be plotted with the age model, and variability in the graph indicated temporal variation in the hydrologic conditions.

3.6. Radiocarbon chronology and the age-depth model

Eight samples were dated using the accelerator mass spectroscopy (AMS) system at the State Key Laboratory of Loess and Quaternary Geology, Institute of Earth Environment, CAS. The AMS ^{14}C data of all of the samples were calibrated using the program CALIB Rev. 7.0.1 with the IntCal13 calibration curve (Reimer et al., 2013). The calibrated median ages were shown as the number of calendar years before present (0 cal yr BP = 1950 AD), and the calendar years were calibrated to their 2σ age ranges (95% probability). The age-depth model was developed through linear interpolation

between the calibrated radiocarbon dates and was presented in Fig. 1.

4. Results

4.1. Core lithostratigraphy and chronology

The stratigraphy of the HE core, summarized in Fig. 1, was complex. The core was visually subdivided into 5 distinct sedimentary units. Unit 1 at the bottom of the core (148–133 cm) consisted of dark grey clay, and the overlying Unit 2 was interpreted as gyttja (133–127 cm) with occasional clay. Dark brownish peat dominated Unit 3 (127–118 cm), which also contained a few marls, and Unit 4 (118–18 cm) consisted almost completely of light brown peat. The uppermost 18 cm (Unit 5) of the core was composed of grass roots exhibiting little decomposition.

The chronology of the HE core was based on eight radiocarbon dates, and details information on the test materials, laboratory number and the calibrated ages can be found in Zhang et al. (2015b) and Wang et al. (2016). The lowermost part of the core was dated to 6000 cal yr BP (Fig. 1), and peat began to accumulate at 4600 cal yr BP (133 cm). The age-depth model suggested a mean sedimentation rate of 0.029 cm/yr, but a notably higher mean peat accumulation rate of 0.038 cm/yr occurred between 3500 and 2300 cal yr BP (128–79 cm).

4.2. The characteristics of the variations in all the proxy data

In this study, we used eight independent proxies for paleohydrology: the DCA axis 1 scores of the plant macrofossils data; charcoal, as counted with a stereoscopic microscope; HD, LOI, grain size and magnetic susceptibility of the sediments; ^{13}C values of *Drepanocladus aduncus*, Equisetaceae and *Carex* roots; and changes in surface wetness expressed as the depth to the water table (DWT), as inferred from changes in testate amoebae assemblages.

DCA is often applied to macrofossil data from wetlands to detect any separations or associations among the taxa (Chiverrell, 2001). In this study, the first DCA axis represents 37.4% of the cumulative variance, which is higher than that the value of the second axis. The main gradient (axis 1) appeared to be related to water level, with a trend from *Carex pseudocuraica* at low values to Equisetaceae at high values and intermediate taxa in the following order: *Carex lasiocarpa*, other *Carex* spp., *Drepanocladus aduncus*, and *Menyanth trifoliata* (Fig. 2). Therefore, the DCA axis 1 scores could be interpreted as a record of water level fluctuations (Fig. 3a). The DCA axis

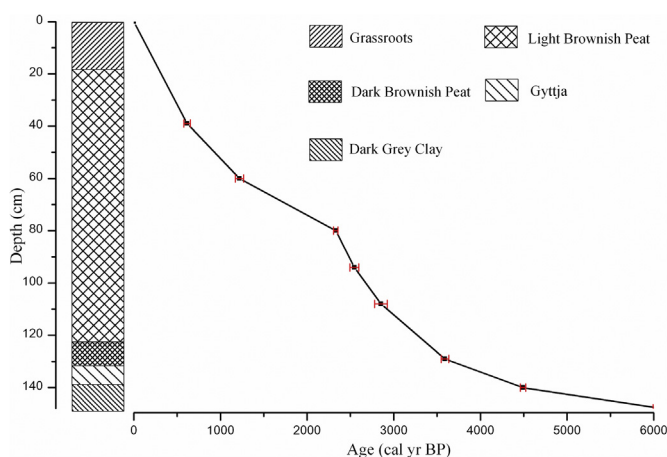


Fig. 1. The sediment units and age-depth model of the core. Model used illustrated by solid line (linear interpolation). AMS radiocarbon dates are shown with the 2 sigma calibrated age by black diamonds. The sediment units were numbered from bottom to uppermost, and the error bar of age was shown by red line. (For interpretation of the references to colour in this figure legend, the reader is referred to the web version of this article.)

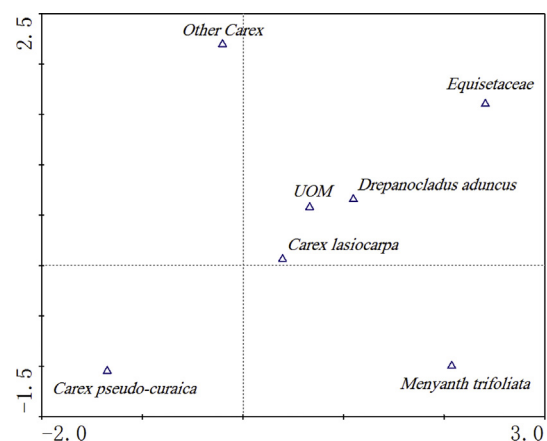


Fig. 2. Biplot of axis 1 and 2 scores from Detrended Correspondence Analysis (DCA) ordination of plant macrofossils from HE profile.

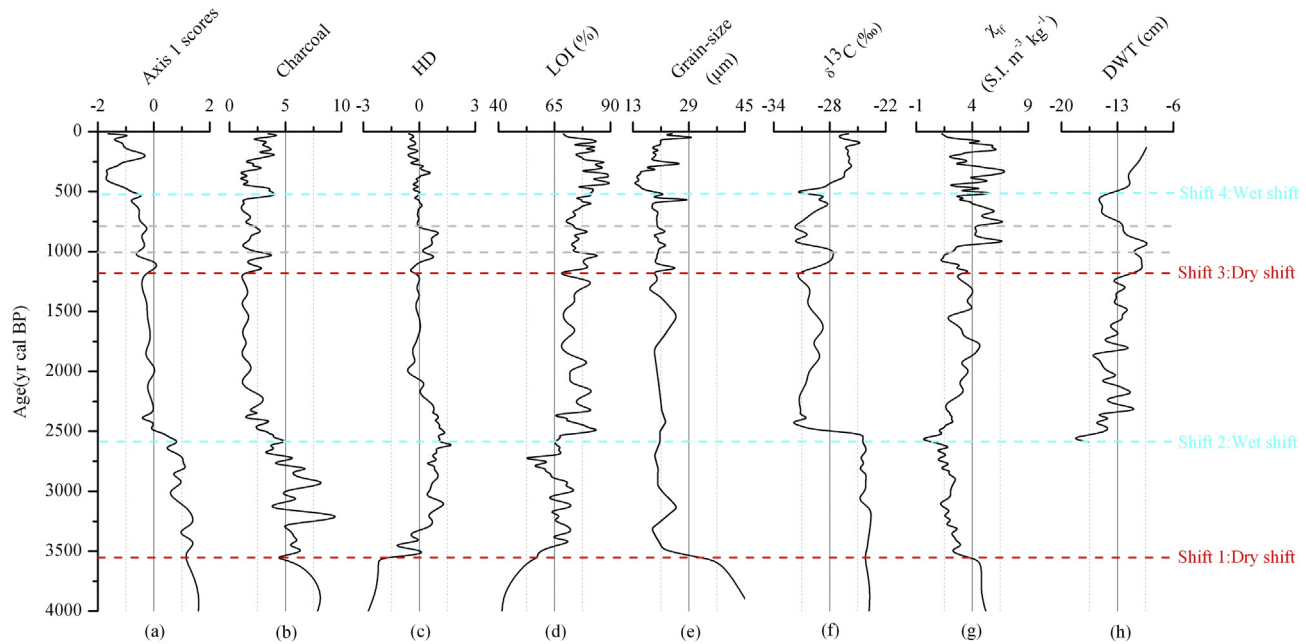


Fig. 3. A summary of the palaeohydrological indices derived from multiple proxies at HE peatland. (a) DCA axis 1 scores from plant macrofossils. (b) The mean values of the absolute numbers of the charcoal counted in both plant macrofossils and pollen samples. (c) The normalised data for humification. (d) LOI expressed as the percentage of the initial weight that burnt away. (e) The mean grain-size of sediments. (f) Stable carbon isotopes of the organic matter. (g) Magnetic susceptibility at low frequency. (h) Mean annual depth to water table (DWT) estimated from testate amoeba assemblages (Song, 2015). The dotted lines in red color marking the dry shifts, and the dotted lines in sky-blue marking the wet shifts. (For interpretation of the references to colour in this figure legend, the reader is referred to the web version of this article.)

1 scores were high from 4000 to 2600 cal yr BP then decreased until 2400 cal yr BP. Then, they showed a dynamically stable pattern with low values from 2400 to 1200 cal yr BP. The axis 1 scores then increased from 1200 to 1100 cal yr BP, remained stable, then sharply declined between 500 and 200 cal yr BP.

Due to its dependence on fire, the production of charcoal (Fig. 3b) could reflect the hydrological conditions of the wetland to some degree (Onac et al., 2015; Patterson Iii et al., 1987). There was a sharp decrease from 4000 to 3600 cal yr BP followed by an increasing trend until the peak of the series at 3200 cal yr BP. The overall production of charcoal then declined until 2400 cal yr BP and maintained consistently low values in a dynamically stable pattern. Production increased between approximately 1200 and 600 cal yr BP, decreased at 500 cal yr BP, and has gradually increased to the present.

Humification represents the level of decomposition of the peat, and changes in the HD is a useful measure of major shifts in surface wetness (Blundell and Barber, 2005). To eliminate the effect of time, the humification data shown in Fig. 3c were detrended. The HD gradually increased from 3600 to 2600 cal yr BP but decreased from 2600 to 2000 cal yr BP before maintaining a dynamically stable pattern from 2000 to 1200 cal yr BP. The HD slowly increased during the period of 1200 to 800 cal yr BP and was dynamically stable from 800 cal yr BP to the present, except for a high value at 300 cal yr BP.

The LOI values of stratigraphic profiles can reflect the organic matter content and accumulated carbon, thus reflecting the hydrologic and thermal conditions and past plant compositions of a wetland (Ma et al., 2009). In this study, the LOI values (Fig. 3d) increased from 4000 to 3400 cal yr BP then fluctuated at approximately 65% during the period of 3400 to 3000 cal yr BP. Subsequently, the LOI declined from 3000 to 2700 cal yr BP before increasing from 2700 to 2400 cal yr BP, after which it maintained a dynamically stable pattern. The LOI was also higher at 400 cal yr BP.

Sediment grain size has been used as an indicator of water level

and paleo-climate, with coarser grains typically interpreted as increasing proximity to shallower water (Campbell, 1998; Digerfeldt, 1986), the heavy precipitation and slumping will transport coarser shallower-water sediments into deeper water. The coarsest particle in sediments is transported by the strongest water movement, and the finest to be deposited being determined by the weakest water movement. Therefore, the grain size of sediments may be a proxy of past climate changes relating to the precipitation (Campbell, 1998). The mean grain size (Fig. 3e) ranged between 13.09 and 44.27 μm , with an average of 20.86 μm . The grain size values decreased from 4000 to 3400 cal yr BP, were low and constant until 1800 cal yr BP, and increased from 1800 to 1500 cal yr BP. The mean grain size values were stable from 1100 to 600 cal yr BP then decreased sharply to the series minimum at 400 cal yr BP. From 400 cal yr BP to the present, the mean grain size exhibited a steeply increasing trend.

The stable carbon isotopes in the HE core ranged from -33.2 to -21.6 ‰, with an average of -27.2 ‰ (Fig. 3f). Previous studies have confirmed that the $\delta^{13}\text{C}$ values of peat plant cellulose can serve as a proxy for climate conditions, with lower $\delta^{13}\text{C}$ values indicating a moister climate and higher $\delta^{13}\text{C}$ values indicating a drier climate (Francey and Farquhar, 1982; Hong et al., 2001). In this study, the $\delta^{13}\text{C}$ values varied between -24.6 and -23.3 ‰ from 4000 to 2500 cal yr BP, followed by a sudden decrease to between -32.3 and -27.3 ‰ from 2500 to 1200 cal yr BP. A sharply oscillating pattern was present from 1200 to 500 cal yr BP, and the $\delta^{13}\text{C}$ values were higher from 500 cal yr BP to the present.

The magnetic susceptibility of the sediment can be used to indicate the hydro-climatic conditions (Reynolds and King, 1995; Verosub and Roberts, 1995). However, several factors can produce variations in the magnetic properties of sediments, for instance, the type of peatland or the concentration of magnetite produced by magnetotactic bacteria in sediment. As Zhong et al. (2010)'s study, wetter climates input relatively coarse clastic materials into runoff, leading to lower χ_{lf} values. At the same time, the concentration of

magnetic detrital input from the catchment will likely increase if there are much rainfall in the region (Williamson et al., 1998). Prasad et al. (2014) have also considered that the low χ_{lf} values may be periods of less rainfall, anoxic conditions or dry periods. As the magnetic susceptibility could be influenced by various factors, it is necessary to combine with other proxies. Factor analysis was made to the initial multi-proxy data, and magnetic susceptibility was in the negative. Therefore, the higher χ_{lf} values indicate wetter climate conditions in this study and vice versa. The magnetic susceptibility of the sediment in this study is presented in Fig. 3g. The χ_{lf} values fluctuated between -0.63×10^{-8} and 7.98×10^{-8} S.I. $m^{-3} kg^{-1}$, with an average value of 3.06×10^{-8} S.I. $m^{-3} kg^{-1}$. The χ_{lf} values decreased from 3600 to 2500 cal yr BP and then gradually increased until 1700 cal yr BP. In the 1700–1200 cal yr BP period, the pattern was dynamically stable. The χ_{lf} reached a low value at 1000 cal yr BP followed by dramatic fluctuations until the present.

The DWT reconstructed from testate amoebae (Fig. 3h) gradually increased from 2600 to 800 cal yr BP and gradually decreased until 500 cal yr BP. It then increased rapidly from 500 cal yr BP to the present (Song, 2015).

4.3. Plant macrofossils and pollen

Fig. 4 presents the plant macrofossils and pollen (expressed as percentages) found in the sedimentary successions over the past 4000 years. These data allowed for a detailed reconstruction of the historical local and regional vegetation. Four main zones were identified based on the cluster analysis of the plant macrofossil and pollen assemblages.

In Zone A (4000–2700 cal yr BP, 131–101 cm), the plant macrofossil assemblages was dominated by *Equisetum fluviatile* and accompanied by low abundances of *Drepanocladus aduncus* and *Menyanthes trifoliata*. The pollen assemblages in this period were

characterized by the highest proportion of herbaceous taxa, which were dominated by *Equisetum*. Similar taxa were also present in the macrofossil record. A low abundance of trees was only observed during 3100–2600 cal yr BP, and the percentage of tree pollen was the lowest in the assemblages during this period. The fern spore pollen mainly consisted of *Aulacomnium*, *Zygetia* and *Mougeotia*.

Zone B (2700–1000 cal yr BP, 101–53 cm) was dominated by *Drepanocladus aduncus* and *Carex lasiocarpa*. Compared to Zone A, the proportion of Equisetaceae decreased slowly in both the plant macrofossil and pollen assemblages, and the beginning of this zone featured a significant increase in *Menyanthes trifoliata*, which reached a maximum at 1800 cal yr BP and then began to fluctuate. The *Aulacomnium* recorded in the pollen reached the highest proportion during this time, and the proportion of trees increased sharply compared to Zone A.

In Zone C (1000–500 cal yr BP, 53–32 cm), the local macrofossils recorded the rapid expansion of *Carex lasiocarpa*, which was the dominant species during this period, while *Drepanocladus aduncus* was always present and exhibited a stable proportion in the sediments. In contrast, the proportion of Equisetaceae decreased continuously in this period. The pollen assemblages in this zone were marked by a sharp increase in trees. Among the trees, *Pinus* was dominant, followed by *Abies*, *Betula*, and *Picea*.

Zone D (500–0 cal yr BP, 32–0 cm) exhibited a significant decline in *Drepanocladus aduncus* and marked increases in *Carex lasiocarpa* and *Carex pseudocuraica*. The recorded wetland herbs included *Menyanthes trifoliata* and Equisetaceae, which were not always present in this zone. This zone featured a higher proportion of trees and a greater abundance of spores which were dominated by *Mougeotia* with a marked increase. The proportion of wetland herbs (for example, *Eriophorum* and *Cyperaceae*) were slightly decreased in this period.

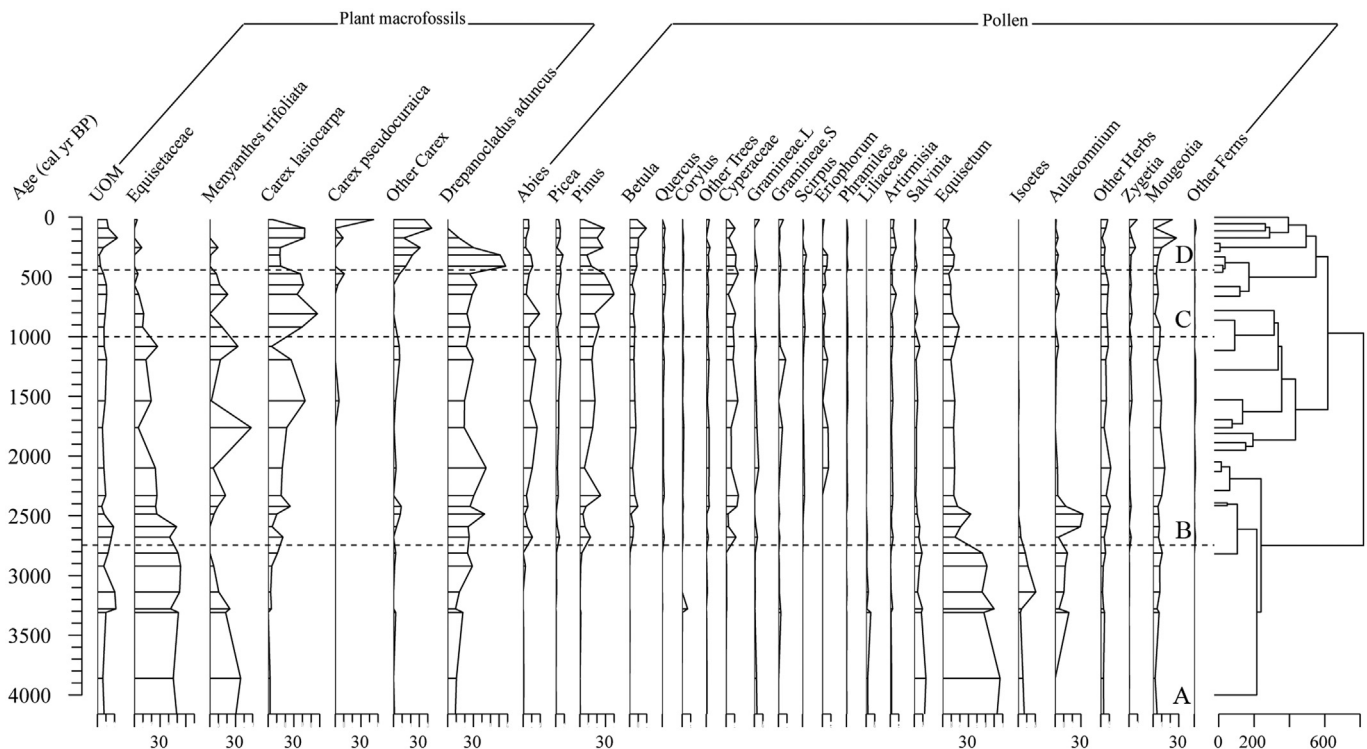


Fig. 4. Percentage plant macrofossils and pollen diagram, all plotted as a percentage of total peat composition (after Wang et al., 2016; Zhang et al., 2015b). Total sum of squares is the result of cluster analysis and four main zones (A/B/C/D) were identified in our data.

4.4. The sensitivity of each proxy

The multi-proxy factor analysis results are presented in Table 1. The data set contained seven variables and 140 sediment samples from the HE core, and two factors explained 69.8% of the total proxy variance. Factor 1 accounted for 45.2% of the total variance and was characterized by high loading of the axis 1 scores (0.897), charcoal (0.855), stable carbon isotopes (0.763) and LOI (0.694). This factor was correlated with biological indicators (except LOI) and was more sensitive to water level changes; thus, positive factor 1 scores indicated a lower water level, while negative scores indicated a higher water level. The variables included in factor 2 accounted for 24.6% of the total variance, and this factor was characterized by high loading of HD (0.893) and magnetic susceptibility (0.795). Factor 2 was exclusively related to physical proxies, and positive scores in factor 2 indicated a lower water level, whereas negative scores indicated a higher water level as well. The variation in the integrated scores from 4000 cal yr BP is presented in Fig. 5.

5. Discussion

5.1. Climatic shifts based on multi-proxy records

The summary diagram (Fig. 3) for the core shows a reconstruction of the surface wetness based on all of the proxy data. Owing to the proxies we used could be reflected many different controlling factors, proxy indicators in multi-proxy studies do not always agree and the differences between them must be critically assessed. In this study, the water level experienced few changes over a long period of time according to the multi-proxy summary plots. As all the proxies were not always in agreement, 'inferred' changes in the water level were identified as discussed below.

At the base of the record at 4000 cal yr BP (130 cm), wet conditions were implied by the low HD and LOI values and high mean grain size and magnetic susceptibility values. This point appeared to represent the start of a wetter phase, which was supported by the decreasing trend in charcoal. However, the stable carbon isotopes remained stable between -25.1 and -23.4 ‰ from 4000 to 2500 cal yr BP. The climate shift apparently left no mark on the abundance of *Equisetum hiemale*, which was the testing material present at the depths of 92 (2500 cal yr BP) to 130 cm (4000 cal yr BP).

A shift to drier conditions (shift 1, Fig. 3) was illustrated by HD, grain size and magnetic susceptibility at approximately 3600 cal yr BP (126 cm). The DCA axis 1 scores, LOI and stable carbon isotopes were high and stable from this point to 2600 cal yr BP (96 cm), suggesting a lower water level during this phase. High values of charcoal were maintained despite the sharp change were existed, implying that this was indeed a period characterized by a lower water level.

A shift to wetter conditions (shift 2, Fig. 3) from 2600 cal yr BP

was implied by a drop in the DCA axis 1 scores and the HD and stable carbon isotope values. A decrease in charcoal showed that the local incidence of fire decreased, indicating that the water level was high. The increasing magnetic susceptibility and DWT also reflected a trend towards greater wetter conditions. However, compared with the previous stage, the LOI had higher values, indicating the opposite conclusion, and the mean grain size was stable during this period. The transport of solid particles may have been driven by other hydrological processes (eg. ripple influences, slumping or turbidity currents), thereby obscuring the climate change signal. What's more, the water level may fall below to the sill after the drier shift (3600 cal yr BP), it would have the effect of imposing a lower sensitivity of grain size to climate.

Almost all of the proxies implied a subsequent major shift to drier conditions (shift 3, Fig. 3) at 1200 cal yr BP. An increase in the DCA axis 1 scores from 1200 cal yr BP (60 cm) coincided with increasing levels of charcoal, HD, LOI and stable carbon isotopes and decreasing levels of magnetic susceptibility. Only the grain size and DWT values increased, suggesting wetter conditions. However, fine grain sizes were present during the period of 900–1100 cal yr BP and the DWT values decreased from 800 to 600 cal yr BP, suggesting a delay in drier conditions.

The testate amoebae transfer function exhibited a rapid shift to wetter conditions (shift 4, Fig. 3) from 500 cal yr BP (31 cm) to the present. The DCA axis 1 scores showed a brief trough at 400 cal yr BP, which was correlated with lower levels of charcoal and HD. The magnetic susceptibility values largely increased in this period, implying that this period did indeed feature a higher water level. However, the LOI was dynamically stable, whereas the stable carbon isotopes sharply increased, and were therefore not in agreement with the other proxies. The LOI factor loading (only 0.694) is the lowest of all the proxies, indicating that we need to be more concerned with other proxies.

Multi-proxy analysis of the history of hydrology in peatland suggested that plant macrofossils, charcoal, stable carbon isotopes, testate amoebae, grain size, LOI, HD and magnetic susceptibility were related. Some general observations can be drawn from this comparison between proxies. The match between HD and magnetic susceptibility is good in terms of the timing of main shifts. However, the value of LOI for 2600 cal yr BP was difficult to interpret the wet shift owing to the increasing of woody plants. The magnitude of organic carbon content is different between herbs and trees. The dry and wet climatic changes fluctuated violently from 1200 to 800 cal yr BP, and the timing of wetness peak in DWT records suggests a delay in drier conditions. One explanation for this is that the testate amoebae records were relatively insensitive to the first drier shift. A major wet shift at 500 cal yr BP presented in five proxies, but their trends were different. Only DWT records and magnetic susceptibility showed a sustainable wetter trend; other proxies showed dynamic trends may be owing to the increasingly enhancement of human activities.

5.2. Relationship between the vegetation and surface wetness

The wetland vegetation succession was affected by various environmental factors, especially the water level. More detailed information on the vegetation changes was revealed by the plant macrofossil and pollen records, and the plant community in the HE core experienced marked transitions in association with the dry-wet changes in climate.

From 4000 to 3200 cal yr BP, the Equisetaceae family, a very common family of hygrophilous plants, was the dominant plant group, and it appeared in both the local and regional vegetation. All of the plants found in the pollen assemblages were moisture-loving herbs, and grasses dominated the plant species. These results

Table 1

Factor analysis matrix after Varimax orthogonal rotation showing the contribution of each proxy identified with Principal Components. We show only the loadings greater than 0.5.

Proxies	Factor 1	Factor 2
DCA Axis 1	0.897	
Charcoal	0.855	
Stable carbon isotope	0.763	
LOI	0.694	
Humification		0.893
Magnetic susceptibility		0.795
Grain size		

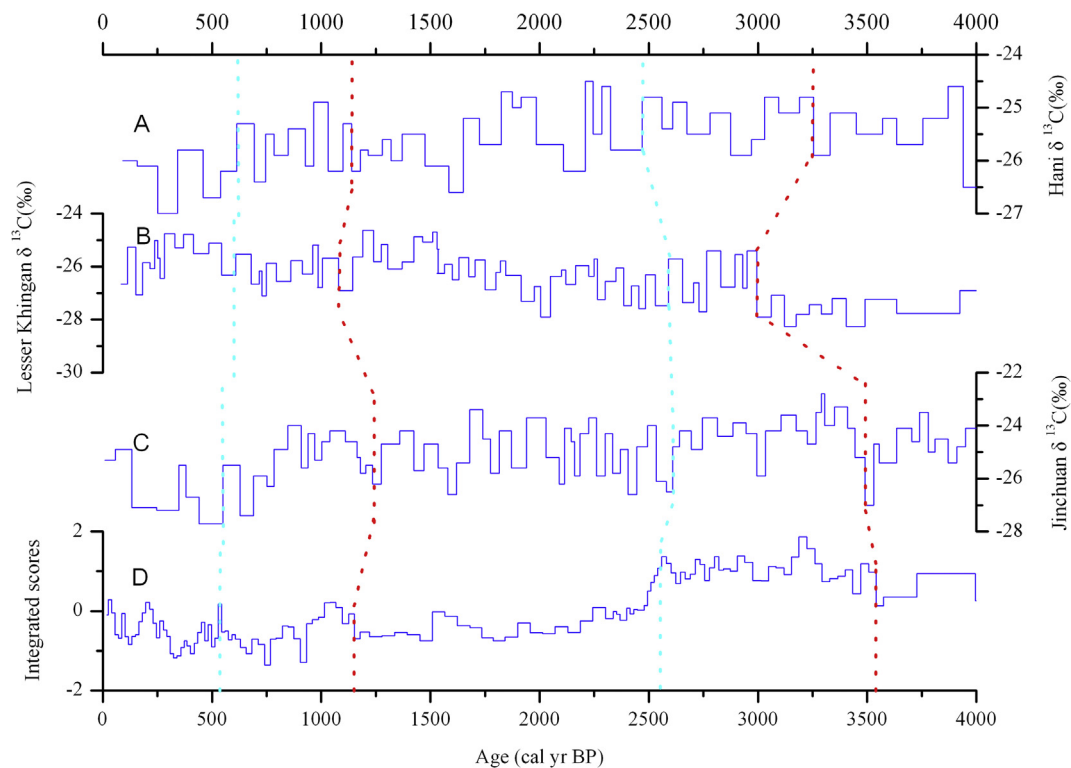


Fig. 5. Comparison with other hydrology records from the Northeast China. A, the $\delta^{13}\text{C}$ records of the plant remain cellulose in the Hani peat bog in the Changbai Mountains (Hong et al., 2005); B, the $\delta^{13}\text{C}$ time series of peat cellulose from Lesser Khingan Mountains (Lin et al., 2004); C, the $\delta^{13}\text{C}$ profile of peat cellulose for the Jinchuan core of the Changbai Mountains (Hong et al., 2001); D, the integrated scores calculated by factor analysis from HE core of the Sanjiang Plain (this study). The dotted lines in red color marking the dry shifts, and the dotted lines in sky-blue marking the wet shifts. (For interpretation of the references to colour in this figure legend, the reader is referred to the web version of this article.)

indicate that this period was rather wet.

At the period of 3200–2400 cal yr BP, the increased abundance of arboreal taxa, especially *Abies*, *Picea*, *Pinus* and *Butula*, was accompanied by a decrease in pollen from most aquatic herbs, such as *Salvinia* and *Isoetes*. These changes reflected a drier period, and the emergence of trees was a sign of a relatively drier climate in the contemporary context of the Sanjiang Plain. Moreover, the rise of arboreal taxa was accompanied by a sharp decrease in Equisetaceae in both the local and regional vegetation, which indicated a drier and warmer climate.

By approximately 2400–1500 cal yr BP, the hydrological condition had changed, and the local vegetation was dominated by *Carex lasiocarpa*, which was accompanied by *Drepanocladus aduncus* and *Menyanthes trifoliata*. The *Carex lasiocarpa* community is also currently dominant in the Sanjiang Plain (Lou and Zhao, 2008). As shown in the pollen diagram, the percent of trees were in lower values, indicating a stage of a wet climate.

There was a decline in *Carex lasiocarpa* from 1500 to 1100 cal yr BP, but the *Menyanthes trifoliata* which had an increasing trend loves moisture better. After that, the *Menyanthes trifoliata* was declined and the *Pinus* was increased in the period of 1100–500 cal yr BP, suggesting a drier condition. The typical wetland plants of carex in the peatland of Sanjiang Plain showed an increasing trend from 500 cal yr BP to the present, and these spores increased remarkably, marking an emergence of moss taxa. It was in accord with the wetter hydrology change in this period.

5.3. Comparison with other hydrologic records from Northeast China

It is difficult to compare different climate records due to

different dating methods (Blundell and Barber, 2005), and differences in the number of radiocarbon dates have led to the application of different age–depth models, which affects the potential for cross-study correlations. However, we attempted to summarize the available peatland climate data to show that there were prominent dry-wet shifts during certain time periods.

As shown in Fig. 3, four proxies indicated that the period from 4000 to 3600 cal yr BP was wetter, and ample evidence from other peat archives also suggested a change in the climate to wetter conditions at approximately 4000 cal yr BP in China (Hong et al., 2010; Huang et al., 2013; Lin et al., 2004; Wang, 1998). Therefore, this shift was highly significant and geographically widespread. The change in wetness may have been due to an abnormal climate event, known as 4.2 ka event (Staubwasser et al., 2003) or the 4.0 ka event during which many extreme floods occurred in northern China (Xia and Yang, 2003).

The shift toward drier conditions recorded at 3600 cal yr BP was supported by evidence from the Jinchuan peatland (Hong et al., 2001) of Changbai Mountains (Fig. 5). Drier conditions lasting for nearly a thousand years (3600–2600 cal yr BP) were also recorded by the hydro-climate records of the Northeast China Summer Monsoon based on the peat cellulose $\delta^{13}\text{C}$ archive found in the Jinchuan peatland (Hong et al., 2001).

The shift toward wetter conditions recorded at 2600 cal yr BP was supported by evidence from the Hanni and Lesser Khingan records presented in Fig. 5. The wet interval deduced from the HE sediments during the 2600–1200 cal yr BP period was strikingly consistent with the climate change inferred from pollen records from northwestern Liaoning Province, Northeast China (Zhang et al., 2004). Evidence for a synchronous shift toward drier conditions at 1100 cal yr BP was found in the Qindeli peatland of the

Sanjiang Plain (Li et al., 2005), but the proposed initiation time was different, which could be due to a difference in dating precision.

The shift toward drier conditions at 1200 cal yr BP was also supported by the three other peat cellulose ^{13}C records in Fig. 5. The period of lower effective precipitation from 1200 to 500 cal yr BP may have been related to the Medieval Warm Period (MWP), although the global nature of this phenomenon remains controversial (Gao et al., 2006).

Abundant evidence in Northeast China supported the existence of a wet climate from 500 cal yr BP to the present (Chu et al., 2009; Wang, 1998; Wu and Shen, 2009; Zhao et al., 2005), but there was also much evidence to support drier conditions during this period (Hong et al., 2001, 2005; Wu et al., 2011). The differences in the site chronologies limited the accuracy and precision of the site-to-site comparisons, particularly at the surface zone. We need a higher resolution age frame (eg. $^{210}\text{Pb}/^{137}\text{Cs}$ dating) to determine the wet-dry shift of recent times next. However, the climate in recent periods appears to be much more complex than that in the past (Waters et al., 2016), the use of a multi-proxy approach may be valuable to assess hydro-climatic changes and to compare the validity of different proxies.

6. Conclusions

We used a multi-proxy approach to reconstruct the peatland surface wetness of the Sanjiang Plain, Northeast China, during the period from 4000 cal yr BP to the present. At 4000 cal yr BP, the peatland conditions were relatively wet, and a rapid and major shift to drier conditions was identified at 3600 cal yr BP. A drier episode was identified at 2600 cal yr BP and was followed by increasing humidity from 2600 to 1200 cal yr BP. Drier conditions were recorded from 1200 to 500 cal yr BP, and the final portion of the records was characterized by wet conditions. The vegetation community transitioned from an *Equisetum fluviatile* community to a *Pinus-Carex lasiocarpa-Drepanocladus aduncus* community followed by a *Pinus-Carex-Mougeotia* community. The results reflected an alternation between drying and wetting in the HE peatland. The biological indicators, such as plant macrofossils, charcoal and stable carbon isotopes, were sensitive to the changes in water level over the last 4000 years, and some of the wet-dry shifts were related to the wetter and drier climate phases inferred from other records. A comparison between the climatic shifts deduced in this study and other climate records from Northeast China suggested that this multi-proxy study provided relatively accurate insights into the paleohydrology, climate and vegetation dynamics, and could be used to inform peatland restoration.

Acknowledgments

The authors gratefully acknowledge the assistance of the Analysis and Test Center of the Northeast Institute of Geography and Agroecology of the Chinese Academy of Sciences. Financial support was provided by the National Natural Science Foundation of China (No.41571191); and the national key research and development project (No.2016YFA0602301). We acknowledge the fruitful comments and many improvements provided by the anonymous reviewers.

References

An, Z., 2000. The history and variability of the East Asian paleomonsoon climate. *Quat. Sci. Rev.* 19, 171–187.
 Argollo, J., Mourguiart, P., 2000. Late quaternary climate history of the Bolivian Altiplano. *Quat. Int.* 72, 37–51.
 Bai, J., Xiao, R., Zhang, K., Gao, H., 2012. Arsenic and heavy metal pollution in wetland soils from tidal freshwater and salt marshes before and after the flow-

sediment regulation regime in the Yellow River Delta, China. *J. Hydrol.* 450, 244–253.
 Baker, A., Caseldine, C.J., Gilmour, M.A., Charman, D., Proctor, C.J., Hawkesworth, C.J., Phillips, N., 1999. Stalagmite luminescence and peat humification records of palaeomisture for the last 2500 years. *Earth Planet. Sci. Lett.* 165, 157–162.
 Barber, K., Chambers, F., Maddy, D., Stoneman, R., Brew, J., 1994. A sensitive high-resolution record of late Holocene climatic change from a raised bog in northern England. *Holocene* 4, 198–205.
 Benvenuto, M.L., Honaine, M.F., Osterrieth, M., Coronato, A., Rabassa, J., 2013. Silicophytoliths in Holocene peatlands and fossil peat layers from Tierra del Fuego, Argentina, southernmost South America. *Quat. Int.* 287, 20–33.
 Blundell, A., Barber, K., 2005. A 2800-year palaeoclimatic record from Tore Hill Moss, Strathspey, Scotland: the need for a multi-proxy approach to peat-based climate reconstructions. *Quat. Sci. Rev.* 24, 1261–1277.
 Bohra, A., Kotlia, B.S., 2015. Tectono-climatic signatures during late quaternary in the Yunam basin, Baralacha Pass (upper Lahaul valley, India), derived from multi-proxy records. *Quat. Int.* 371, 111–121.
 Buckley, D.E., Smith, J.N., Winters, G.V., 1995. Accumulation of contaminant metals in marine sediments of Halifax Harbour, Nova Scotia: environmental factors and historical trends. *Appl. Geochem.* 10, 175–195.
 Campbell, C., 1998. Late Holocene lake sedimentology and climate change in Southern Alberta, Canada. *Quat. Res.* 49, 96–101.
 Chambers, F.M., Charman, D.J., 2004. Holocene environmental change: contributions from the peatland archive. *Holocene* 14, 1–6.
 Charman, D.J., Hendon, D., Packman, S., 1999. Multiproxy surface wetness records from replicate cores on an ombrotrophic mire: implications for Holocene palaeoclimate records. *J. Quat. Sci.* 14, 451–463.
 Chiverrell, R., 2001. A proxy record of late Holocene climate change from May Moss, northeast England. *J. Quat. Sci.* 16, 9–29.
 Chu, G., Sun, Q., Wang, X., Li, D., Rioual, P., Qiang, L., Han, J., Liu, J., 2009. A 1600 year multiproxy record of paleoclimatic change from varved sediments in Lake Xiaolongwan, Northeastern China. *J. Geophys. Res. Atmos.* 114, 2191–2196.
 Davis, J.C., Sampson, R.J., 1986. *Statistics and Data Analysis in Geology*. Wiley, New York.
 Digerfeldt, G., 1986. *Studies on Past Lake-level Fluctuations*. Wiley, New York.
 Elliott, S.M., Roe, H.M., Patterson, R.T., 2012. Testate amoebae as indicators of hydroseral change: an 8500 year record from Mer Bleue Bog, eastern Ontario, Canada. *Quat. Int.* 268, 128–144.
 Faegri, K., Kaland, P.E., Krzywinski, K., 1989. *Textbook of Pollen Analysis*. Wiley, New York.
 Francey, R.J., Farquhar, G.D., 1982. An explanation of $^{13}\text{C}/^{12}\text{C}$ variations in tree rings. *Nature* 297, 28–31.
 Gao, J., Liu, J., Wang, S., 2006. Overview on studies of Medieval warm period in China. *Sci. Geogr. Sin.* 26, 376–383 (In Chinese).
 Heiri, O., Lotter, A.F., Lemcke, G., 2001. Loss on ignition as a method for estimating organic and carbonate content in sediments: reproducibility and comparability of results. *J. Paleolimnol.* 25, 101–110.
 Henderson, A.C.G., Holmes, J.A., 2009. Palaeolimnological evidence for environmental change over the past millennium from Lake Qinghai sediments: a review and future research perspective. *Quat. Int.* 194, 134–147.
 Hong, B., Hong, Y.T., Lin, Q.H., Shibata, Y., Uchida, M., Zhu, Y.X., Leng, X.T., Wang, Y., Cai, C.C., 2010. Anti-phase oscillation of Asian monsoons during the younger dryas period: evidence from peat cellulose delta C-13 of Hani, Northeast China. *Palaeogeogr. Palaeoclimatol. Palaeoecol.* 297, 214–222.
 Hong, Y.T., Hong, B., Lin, Q.H., Shibata, Y., Hirota, M., Zhu, Y.X., Leng, X.T., Wang, Y., Wang, H., Yi, L., 2005. Inverse phase oscillation between the East Asian and Indian ocean summer monsoons during the last 12000 years and paleo El Niño. *Earth Planet. Sci. Lett.* 231, 337–346.
 Hong, Y.T., Wang, Z.G., Jiang, H.B., Lin, Q.H., Hong, B., Zhu, Y.X., Wang, Y., Xu, L.S., Leng, X.T., Li, H.D., 2001. A 6000-year record of changes in drought and precipitation in northeastern China based on a C-13 time series from peat cellulose. *Earth Planet. Sci. Lett.* 185, 111–119.
 Huang, T., Cheng, S., Mao, X., Hong, B., Hu, Z., Zhou, Y., 2013. Humification degree of peat and its implications for Holocene climate change in Hani peatland, Northeast China. *Chin. J. Geochem.* 32, 406–412 (In Chinese).
 Janssens, J.A., 1983. A quantitative method for stratigraphic analysis of bryophytes in holocene peat. *J. Ecol.* 71, 189–196.
 Kaiser, H.F., 1960. The application of electronic computers to factor analysis. *Educ. Psychol. Meas.* 20, 141–151.
 Kotlia, B.S., Sanwal, J., Phartiyal, B., Joshi, L.M., Trivedi, A., Sharma, C., 2010. Late Quaternary climatic changes in the eastern Kumaun Himalaya, India, as deduced from multi-proxy studies. *Quat. Int.* 213, 44–55.
 Lejju, J.B., 2009. Vegetation dynamics in western Uganda during the last 1000 years: climate change or human induced environmental degradation? *Afr. J. Ecol.* 47, 21–29.
 Li, X., Zhao, H., Yan, M., Wang, S., 2005. Fire variations and relationship among fire and vegetation and climate during Holocene at Sanjiang Plain, Northeast China. *Sci. Geogr. Sin.* 25, 177–182 (In Chinese).
 Lin, Q., Leng, X., Hong, B., 2004. Peat C-13 record of climate change in Xiao Xingganling in the past 5000 years. *Earth Environ.* 32, 50–54.
 Liu, H., Gao, C., Yu, X., Zhang, Z., Wang, G., 2016. The prospects in studying reference conditions constructing of ecological restoration of wetlands based on paleoecological records. *Wetl. Sci.* 14, 568–575 (In Chinese).
 Liu, X., Ma, X., 2000. Influence of large-scale reclamation on natural environment and regional environmental protection in the sanjiang plain. *Sci. Geogr. Sin.* 01,

- 14–19 (In Chinese).
- Liu, X., Ma, X., 2002. Natural Environmental Changes and Ecological Protection in the Sanjiang Plain. Science press, Beijing.
- Lou, Y.J., Zhao, K.Y., 2008. Analysis of interspecific associations of *Carex lasiocarpa* community in recent 30-year succession in Sanjiang Plain. *Chin. J. Ecol.* 27, 509–513 (In Chinese).
- Lu, H., An, Z., 1998. Paleoclimatic significance of grain size of loess-palaeosol deposit in Chinese Loess Plateau. *Sci. China* 41, 626–631 (In Chinese).
- Ma, C.M., Cheng, Z., Zheng, C.G., Qian, Y., Zhao, Z.P., 2009. Climate changes in East China since the Late-glacial inferred from high-resolution mountain peat humification records. *Sci. China* 52, 118–131 (In Chinese).
- Mansell, L.J., Whitehouse, N.J., Gearey, B.R., Barratt, P., Roe, H.M., 2014. Holocene floodplain palaeoecology of the Humberhead Levels; implications for regional wetland development. *Quat. Int.* 341, 91–109.
- Onac, B.P., Hutchinson, S.M., Geanta, A., Forray, F.L., Wynn, J.G., Giurgiu, A.M., Coroiu, I., 2015. A 2500-yr late Holocene multi-proxy record of vegetation and hydrologic changes from a cave guano-clay sequence in SW Romania. *Quat. Res.* 83, 437–448.
- Patterson Iii, W.A., Edwards, K.J., Maguire, D.J., 1987. Microscopic charcoal as a fossil indicator of fire. *Quat. Sci. Rev.* 6, 3–23.
- Pawlowski, D., Milecka, K., Kittel, P., Woszczyk, M., Szychalski, W., 2015. Palaeoecological record of natural changes and human impact in a small river valley in Central Poland. *Quat. Int.* 370, 12–28.
- Plunkett, G., Swindles, G.T., 2008. Determining the Sun's influence on Lateglacial and Holocene climates: a focus on climate response to centennial-scale solar forcing at 2800 cal. BP. *Quat. Sci. Rev.* 27, 175–184.
- Prasad, V., Farooqui, A., Sharma, A., Phartiyal, B., Chakraborty, S., Bhandari, S., Raj, R., Singh, A., 2014. Mid-late Holocene monsoonal variations from mainland Gujarat, India: a multi-proxy study for evaluating climate culture relationship. *Palaeogeogr. Palaeoclimatol. Palaeoecol.* 397, 38–51.
- Reimer, P.J., Bard, E., Bayliss, A., Beck, J.W., Blackwell, P.G., Ramsey, C.B., Buck, C.E., Cheng, H., Edwards, R.L., Friedrich, M., 2013. Intcal 13 and marine 13 radiocarbon age calibration curves 0–50,000 years cal BP. *Radiocarbon* 55, 1869–1887.
- Reynolds, R.L., King, J.W., 1995. Magnetic records of climate change. *Rev. Geophys.* 33, 101–110.
- Santisteban, J.I., Mediavilla, R., López-Pamo, E., Dabrio, C.J., Zapata, M.B.R., García, M.J.G., Castaño, S., Martínez-Alfaro, P.E., 2004. Loss on ignition: a qualitative or quantitative method for organic matter and carbonate mineral content in sediments? *J. Paleolimnol.* 32, 287–299.
- Shen, J., Liu, X., Wang, S., Matsumoto, R., 2005. Palaeoclimatic changes in the Qinghai Lake area during the last 18,000 years. *Quat. Int.* 136, 131–140.
- Song, L., 2015. Biodiversity of Testate Amoebae and Their Indicating Role in Palaeohydrological Reconstruction in Peatland in Sanjiang Plain. Northeast Institute of Geography and Agroecology, Chinese Academy of Sciences, University of Chinese Academy of Sciences, Changchun. (In Chinese).
- Staubwasser, M., Sirocko, F., Grootes, P., Segl, M., 2003. Climate change at the 4.2 ka BP termination of the Indus valley civilization and Holocene south Asian monsoon variability. *Geophys. Res. Lett.* 30, 1–4.
- Verosub, K.L., Roberts, A.P., 1995. Environmental magnetism: past, present, and future. *J. Geophys. Res. Atmos.* 100, 411–413.
- Wang, C., Zhao, H., Wang, G., 2015. Vegetation development and water level changes in Shenjiadian peatland in Sanjiang Plain, Northeast China. *Chin. Geogr. Sci.* 25, 451–461.
- Wang, C., Zhao, H., Yu, X., Lu, X., Wang, G., 2016. Palaeovegetation of Honghe wetland in Sanjiang Plain as a basis for conservation management and restoration. *Ecol. Eng.* 96, 79–85.
- Wang, Z., 1998. Reconstruction of past 5000-year humidity changes of Northeast China using C-13 values of peat cellulose in Jinchuan region, Jilin Province. *Bull. Mineral., Petrol. Geochem.* 17, 54–56.
- Waters, C.N., Zalasiewicz, J., Summerhayes, C., Barnosky, A.D., Poirier, C., Galuszka, A., Cearreta, A., Edgeworth, M., Ellis, E.C., Ellis, M., Jeandel, C., Leinfelder, R., McNeill, J.R., Richter, D.D., Steffen, W., Syvitski, J., Vidas, D., Wagreich, M., Williams, M., An, Z.S., Grinevald, J., Odada, E., Oreskes, N., Wolfe, A.P., 2016. The Anthropocene is functionally and stratigraphically distinct from the Holocene. *Science* 351, 137.
- Williamson, D., Jelinowska, A., Kissel, C., Tucholka, P., Gibert, E., Gasse, F., Massault, M., Taieb, M., Van Campo, E., Wieckowski, K., 1998. Mineral-magnetic proxies of erosion/oxidation cycles in tropical maar-lake sediments (Lake Tritrivakely, Madagascar): paleoenvironmental implications. *Earth Planet. Sci. Lett.* 155, 205–219.
- Wu, J., Shen, J., 2009. Paleoenvironmental and paleoclimatic changes reflected by diffuse reflectance spectroscopy and magnetic susceptibility from Xingkai Lake sediments. *Mar. Geol. Quat. Geol.* 29, 123–131.
- Wu, J., Wang, Y., Dong, J., 2011. Changes in East Asian summer monsoon during the holocene recorded by stalagmite O-18 records from Liaoning Province. *Quat. Sci.* 31, 990–998 (In Chinese).
- Xia, Z., Yang, X., 2003. Preliminary study on the flood events about 4 ka BP in north China. *Quat. Sci.* 23, 667–674.
- Zhang, X., Li, Y., Liu, G., Yin, H., 2004. Environmental change in the northwest area of Liaoning province during the middle holocene. *Mar. Geol. Quat. Geol.* 24, 115–120 (In Chinese).
- Zhang, Z., Xing, W., Lv, X., Wang, G., 2014. The grain-size depositional process in wetlands of the Sanjiang Plain and its links with the East Asian monsoon variations during the Holocene. *Quat. Int.* 349, 245–251.
- Zhang, Z., Xing, W., Wang, G., Tong, S., Lv, X., Sun, J., 2015a. The peatlands developing history in the Sanjiang Plain, NE China, and its response to East Asian monsoon variation. *Sci. Rep.* 5, 1–10.
- Zhang, Z., Zhong, J., Lv, X., Tong, S., Wang, G., 2015b. Climate, vegetation, and human influences on late-Holocene fire regimes in the Sanjiang plain, northeastern China. *Palaeogeogr. Palaeoclimatol. Palaeoecol.* 438, 1–8.
- Zhao, H., Wang, S., Zhou, D., 2005. Peat record of climate change in the Dunhua basin, Jilin Province since 2200 a BP. *J. Northeast Normal Univ. (Nature Science Edition)* 37, 111–115 (In Chinese).
- Zhong, W., Xue, J., Ouyang, J., Zheng, Y., Ma, Q., Yu, X., 2010. Last glacial climate variations on the tropical Leizhou Peninsula, South China. *J. Paleolimnol.* 44, 777–788.